RISØ

Risø-R-477

Risø-R-477

Biological Effectiveness and Application of Heavy Ions in Radiation Therapy described by a Physical and Biological Model

Kjeld J. Olsen and Johnny W. Hansen

Risø National Laboratory, DK-4000 Roskilde, Denmark
December 1982

RISØ-R-477

BIOLOGICAL EFFECFIVENESS AND APPLICATION OF HEAVY IONS IN RADIATION THERAPY DESCRIBED BY A PHYSICAL AND BIOLOGICAL MODEL

Kjeld J. Olsen[x] and Johnny W. Hansen

[x]Department of Radiophysics
Copenhagen University Hospital, Herlev
DK-2730 Herlev

Abstract. A description is given of the physical basis for applying track structure theory in the determination of the effectiveness of heavy-ion irradiation of single- and multi-hit target systems.

It will be shown that for applying the theory to biological systems the effectiveness of heavy-ion irradiation is inadequately described by an RBE-factor, whereas the complete formulation of the probability of survival must be used, as survival depends on

(continue on next page)

December 1982
Risø National Laboratory, DK-4000 Roskilde, Denmark

both radiation quality and dose. The theoretical model of track structure can be used in dose-effect calculations for neutron-, high-LET, and low-LET radiation applied simultaneously in therapy.

INIS descriptors: BIOLOGICAL RADIATION EFFECTS; DOSE-RESPONSE RELATIONSHIPS; DOSEMETERS; FRACTIONATED IRRADIATION; HEAVY IONS; IONIZING RADIATIONS; LET; MICRODOSIMETRY; NUCLEAR EMULSIONS; OXYGEN ENHANCEMENT RATIO; PARTICLE TRACKS; RADIATION DETECTORS; RADIATION QUALITY; RADIOTHERAPY; RBE; SURVIVAL CURVES

UDC 537.534 : 615.849

This work is based on lectures in the Department of Radiophysics and Oncology at Copenhagen University Hospital, Herlev.

ISBN 87-550-0886-0
ISSN 0106-2840

Risø Repro 1983

CONTENTS

1. INTRODUCTION

Clinical experience in radiotherapy is based on the use of low-LET radiation in which the absorbed dose is a sufficient description of the radiation field. In the case of high-LET radiation such as neutrons, heavy ions, and π-mesons we have a completely different situation since the radiation field now consists of a distribution in energy and particle type. Primary and secondary ions, secondary electrons, and gamma-radiation will interact differently with the dose meter or tissue being irradiated and thus contribute to the total effect in a very complex way. The result is that measurement of the absorbed dose no longer suffices to predict the effect that we are seeking, as a one-to-one correspondence between dose and its effect no longer exists. Use of simple conversion factors like RBE for calculating the effect of a given dose is not a particularly useful method and in most cases it will give the wrong result.

Even where it is merely a question of correlating dose and effect proportionately the situation quickly gets complicated since one must correct for the particle type, energy spectrum of the particles, as well as tissue type. In short, for high-LET irradiation isodose contours are isoeffect contours only if the particle spectrum remains constant. Further, the dose-effect curve will vary with materials and particles.

When speaking of the response of a detector or tissue to ionizing radiation of various types or qualities we use a concept called the relative biological effectiveness, RBE for short, and express it as a function of LET, as shown in Fig. 1. RBE is given as the ratio of the dose of low-LET radiation, usually with 200 kVp x-rays as reference, to that of high-LET radiation necessary to produce the same effect. The curves in Fig. 1 show clearly that different biological systems display a marked variation in their RBE-LET characteristic with the value of LET for maximum RBE varying by a factor of 10 from one system to the other. Further, cells show initially an increase in RBE with

increasing LET followed by a decrease at very high LET, whereas the bacteria systems like most physical detectors display a monotonically decrease in RBE with increasing LET and with RBE always less than unity. This leads to the impossibility of distinguishing between low- and high-LET radiation without specifying the material under irradiation. In other words, LET is not a useful parameter for describing the sensitivity of different materials to ionizing radiation. We must instead start looking for better parameters to distinguish low- from high-LET radiation.

2. GENERAL DESCRIPTION OF THE TRACK STRUCTURE THEORY

The track structure theory has been developed to describe the blackness of photographic emulsions around the path of a heavy particle. Photographic emulsions consist of silver halide crystals embedded in a gelatine base. Various chemicals may be added in ppm-amounts to alter the sensitivity of the emulsion sharply. An example of a heavy ion emulsion track is shown in Fig. 2. It is evident that the track is very irregular and in the beginning the developed grains are very scattered while only at the end of the particle range, where the ion has given up almost all its energy, is the track continuous. The first irregular part is in many respects analogous to the cluster theory[1)] in radiation chemistry. This theory considers the interaction between radiation and matter to occur in discrete steps with about 50-100 eV deposited in a cluster of excited and ionized atoms or molecules. The radiation effects arise from reactions in the clusters and the diffusion of reactive species, mainly radicals from the clusters. LET gives only the mean distance between clusters and no indication of their spatial distribution, which again points to the poor predictive value of LET.

The silver halide crystals are about 0.2 μm in average physical

dimension; with a density of about 9 this corresponds to about 2 μm at unit density. The photographic emulsion may be thought of as a matrix of radiation-sensitive elements each consisting of a silver halide crystal responding to the average dose to the element.

In the case of biological systems the sensitive element is usually assumed to be the cell nucleus which has a diameter of a few μm, i.e. approx. the same as the silver halide crystal at unit density. It may be more correct to consider the DNA molecule as the sensitive element. DNA is very twisted and, except at cell mitosis, bound to the cell membrane. The size of DNA as the sensitive element is not well defined; another complication is that energy can move extensively within the DNA molecule up to several hundreds of base pairs from where the energy originally was deposited.

In physical detectors the sensitive element may vary in size from that of a single molecule, e.g. the dye film dose meter, up to several nm in cases where collective phenomena play a role as they do in scintillator solutions.

The response of physical and biological systems to low-LET radiation may often be described by a multi-hit model which includes a parameter m that may be thought of as a measure of the number of times the sensitive element must be hit by an electron which deposits energy in the element. In track structure theory m is called the "hittedness".

Photographic emulsions may vary from 1- to 8-hit detectors according to the chemical nature of the additives or the use of various development procedures, and may thus mimic various biological as well as physical systems. The probability for activation of a sensitive element can be described by Poisson statistics with P = activation probability = $[1- \exp(-D/D_{37})]^m$. D_{37} is a characteristic dose corresponding to each element receiving one hit on the average, while m is the hittedness of the detector. Some detectors like LiF-TLD show a mixed 1- and 2-hit response.

1-hit response is characteristic of most physical detectors. An ideal 1-hit detector has the following properties: 1) a linear dose response up to doses comparable to D_{37}, 2) absence of dose-rate effects since the sensitive element may be activated by a single electron, and fading or repair is disregarded, 3) in a log-log plot all dose-response curves will be 45° lines no matter if the radiation is of high- or low-LET, and 4) RBE will decrease monotonically with LET as shown in Fig. 1 for bacteria. For a 1-hit detector where activation may be brought about by a single electron passing through the element, RBE must always be less than or equal to unity.

In less-sensitive photographic emulsions the silver halide crystal must be hit more than once by electrons, resulting in a supralinear dose-response for low-LET radiation. An example of this is shown in Fig. 3. The figure closely resembles a survival curve for biological systems and indicates that physical detectors suitably chosen may be used to study radiation effects on biological systems, e.g. at low doses.

In the case of multi-hit detectors, i.e. with $m \geq 2$ RBE may be both larger and smaller than 1 depending on LET. By concentrating the absorbed energy on a small area around the particle track RBE may become greater than one. If the concentration becomes too high, i.e. the dose surpasses D_{37}, RBE starts to fall due to an overkill effect as may also be seen from the Poisson statistics. This describes the variation of RBE in cell systems with LET as shown in Fig. 1.

The study of heavy ion tracks in a photographic emulsion, as shown in Fig. 2, has led Katz and coworkers[2] to distinguish between two types of activation processes: "gamma-kill" and "ion-kill". Gamma-kill designates an activation of the sensitive element arising from hits by electrons from low-LET radiation or δ-rays produced by different ions. Thus there is no spatial or temporal correlation between the electrons that hit the sensitive element.

In the ion-kill mode the element is activated directly by the

ion passing through it or else the ion passes so close to the element that it is inactivated by the tangle of δ-rays emanating from the particle track. Gamma-kill is possible only with a beam of particles and the probability of gamma-kill will depend on the density of particles and thus on dose. At low doses gamma-kill will be very unlikely since the mean density of electrons decreases in proportion to the dose, whereas the probability for gamma-kill will vary with D^m, m being the hittedness.

The distinction between the two inactivation modes is mainly that ion-kill relates to a single particle where the probability for the effect is described by a cross-section. For a particle-beam the number of sensitive elements inactivated by ion-kill will vary in direct proportion to the dose, since the number of particles decreases linearly with dose. According to this point of view, a single electron cannot lead to ion-kill. Thus there will be no effect of a single electron passing through a multi-hit detector.

The tracks of heavy ions shown in Fig. 2 are due to ion-kill. The irregular part of the track is called "grain-count", while the continuous portion is called "track-width". Grain-count is typical for fast heavy ions with low charge, e.g. protons, while track-width is encountered with ions of low velocity and high effective charge and correspondingly high LET.

3. DESCRIPTION OF THE THEORETICAL MODEL

The track structure theory as developed by Katz and coworkers[3] is based on the often overlooked fact that regardless of the primary type of radiation, whether gamma- or x-rays, electrons, neutrons, heavy particles or π-mesons, the interaction between radiation and matter is mediated via secondary or higher-order electrons.

For purposes of calculation the detectors are assumed to be much more sensitive towards ionization than excitation, i.e. they are relatively insensitive to uv irradiation. This is the case for most physical detectors and almost all biological systems[4].

To get a better understanding of the secondary electron spectrum, we must look at the ionization cross-section as a function of the energy. This is shown in Fig. 4. From the figure it is evident that the two curves for molecular hydrogen and mercury are almost identical despite their large difference in atomic number.

Typically, a lower limit for ionization is observed around 10 eV with a maximum value for the cross-section at 100 eV followed by a slow decrease to almost zero at 10 keV. This indicates that the main part of the ionization is caused by electrons in the energy range 10 eV to 10 keV.

Figure 5 shows the slowing-down spectrum in aluminium of ^{64}Cu and ^{198}Au β-rays of 0.57 and 0.96 MeV maximum energy, respectively. Despite the large difference in initial energy the spectra are almost identical below 10 keV. This indicates that as long as the primary energy of the electrons is large compared with 10 keV the shape of the slowing-down spectrum for low energies will be independent of the primary source of the electrons.

The detector response, which is proportional to the product of the spectrum for the ionization cross-section and the spectrum for slowing down of the electrons, must be the same for every type of low-LET radiation as long as the reference radiation with which it is compared has an energy considerably higher than 10 keV.

The conclusion to be drawn from this is that radiation effects of low-energy electrons will be identical to damage from every other type of low-LET radiation. Thus the problem of effectiveness of high-LET radiation concentrates on finding the dose

distribution around the particle track. The calculated dose distribution may then be converted to a distribution of radiation effects when the dose-response characteristics of the detector are known from experiments with low-LET radiation.

The shape of the dose-response curve for a system irradiated with gamma-rays is of great importance for determining this curve for various types of high-LET radiation. The dose-response curve for gamma-rays is used to translate the radial distribution of dose around the ion track into a radial distribution of the probability for the effect.

Damage at low doses will typically be important at radial distances of up to 0.1 μm from the center of the ion path. In this range the dose will be high and possibly surpass the characteristic dose. The relation of the energy deposited in the high-dose area near the ion track to the total energy deposited is of prime importance in determining the effectiveness of various radiation qualities.

If the dose-response curve for gamma-rays is purely exponential the dose response for any ionizing radiation will also be exponential and RBE will never exceed unity, according to particle track structure theory. If the survival curve for gamma-radiation exhibits a shoulder, the shape of the dose-response curve may be different for other kinds of radiation qualities and RBE may be greater than unity. This last situation is much more complex and will be the subject of a later section.

The description of the track structure model will initially be restricted to 1-hit detectors since computationally they are less complicated, but the principles are identical for multi-hit detectors.

In the model it is assumed that the detectors consist of radiation-sensitive elements in the shape of small cylinders with diameter and length equal to $2a_0$ and with the cylinder axis parallel to the particle track at a distance t from the center of the track as shown in Fig. 6.

With the cylinders placed as shown they will experience a strongly varying dose around the track of the ion, but for the determination of damage the mean dose to the cylinder must be calculated.

The distribution of dose around the track may be calculated from the Bethe equation which gives the number of δ-rays per unit energy interval and per unit path length along the particle track in connection with a formalism for the energy deposition or range-energy relation of low-energy electrons. Without going into detail the dose distribution may be calculated from

$$\bar{D}_\delta(z,\beta,t,a_o) = \frac{1}{\pi a_o^2} \int_{t-a_o}^{t+a_o} D_\delta(z,\beta,t) \cdot A(a_o,t)\,dt \qquad (1)$$

with

$$D_\delta(z,\beta,t) = \frac{1}{2\pi t dt} \int_{\omega_t}^{\omega_{max}} \frac{dn(\omega_r)}{d\omega_r} \cdot \frac{d\omega_{r-t}}{dt}\, d\omega \; . \qquad (2)$$

$\bar{D}_\delta(z,\beta,t,a_o)$ is the average dose to a sensitive element of radius a_o placed at a distance t from the path of the moving ion of effective charge z and velocity β relative to the velocity of light. $A(a_o t)$ is a geometrical factor determined by the size and position of the sensitive element at a distance t from the particle track. $(2\pi t dt)^{-1}$ is a volume element per unit path length along the track, $\frac{d\omega_{r-t}}{dt}$ the stopping power for δ-rays, and $\frac{dn(\omega_r)}{d\omega_r}$ the energy distribution of δ-rays given by the Bethe equation:

$$\frac{dn(\omega_r)}{d\omega_r} = \frac{2\pi N e^4}{mc^2} \cdot \frac{z_{eff}^2}{\beta^2} \cdot \frac{1}{\omega_r^2} \; . \qquad (3)$$

N is the number of free electrons per unit volume in the detector, e and m the charge and mass of the electron, c the velocity of light, z_{eff} the effective charge of the ion, and β the velocity of the ion relative to that of light.

The Bethe equation is invalid at small ranges, i.e. at low electron energies, where binding effects play a role. This problem may be avoided by considering separately an area of radius a_0 with the center placed at the center of the path of the ion. The total energy deposited by the δ-rays with range exceeding a_0 is calculated from the Bethe equation. The energy deposited in the core, i.e. the central element, may be found as the difference between the total energy loss per unit path length given by the LET and the energy deposited in the track, i.e. in the area outside the central element of radius a_0.

It will take us too far to go into the details of the calculations of the dose distribution, but the calculated mean dose to the sensitive element $\bar{D}\beta^2/z_{eff}^2$ normalized with respect to $z_{eff}^2\beta^{-2}$ is shown in Fig. 7 as a function of the distance t from the center of the track. From this figure it follows that 1) for distances $t < a_0$, i.e. within the core, $\bar{D}$ varies in proportion to $z_{eff}^2\beta^{-2}a_0^{-2}$, or that the mean dose in the core is inversely proportional to the square of the radius of the sensitive element, and 2) for $t > 3a_0$ the dose varies with $z_{eff}^2\beta^{-2}t^{-2}$ such that the mean dose $\bar{D}$ is independent of the size of the sensitive element at distances greater than 3 times the radius of the sensitive element. In all cases the mean dose varies with $z_{eff}^2\beta^{-2}$, which points to $z_{eff}^2\beta^{-2}$ as an important parameter.

The effect of the dose will be described as already indicated by the Poisson equation:

$$P(z,\beta,t,a_0) = 1 - \exp(-\bar{D}(z,\beta,t,a_0)/D_{37}), \qquad (4)$$

with $\bar{D}(z,\beta,t,a_0)$ as the mean dose to a sensitive element at a

distance t from the track. $P(z,\beta,t,a_0)$ denotes the fraction of sensitive elements lying at a distance t from the track that is inactivated by the incoming ion.

The total effect is calculated by integration of the probability from t = 0 to the maximum range of the δ-rays. This integration gives the probability (i.e., cross-section) for inactivation

$$\sigma_T(z,\beta,a_0) = 2\pi \int_0^{t_{max}} P(z,\beta,t,a_0)\,t\,dt \ . \qquad (5)$$

The sensitivity of a detector towards heavy ions is defined as the ratio of the total cross-section σ_T to the total energy E_T deposited, while the sensitivity of the detector to low-LET radiation is given by $1/D_{37}$. The relative biological effectiveness, RBE, defined as the ratio of the sensitivities, is given by

$$\text{Sensitivity to low-LET} \qquad k_\gamma = 1/D_{37} \qquad (6)$$

$$\text{Sensitivity to heavy ions} \qquad k_i = \sigma_T/E_T \qquad (7)$$

$$\text{RBE} = \frac{k_i}{k_\gamma} = \frac{\sigma_T \cdot D_{37}}{E_T} \qquad (8)$$

The total energy deposited in a volume element, V, may be expressed as $E_T = V \cdot \bar{D}$ assuming unit density. A Taylor expansion of the exponential term in the expression for $P(z,\beta,t,a_0)$ gives

$$P(z,\beta,t,a_0) \simeq \bar{D}/D_{37} - \tfrac{1}{2}(D/D_{37})^2 + \ldots\ldots , \qquad (9)$$

which shows that for values of $D \ll D_{37}$, σ_T is given by

$\sigma_T \simeq \bar{D}/D_{37}$ to a good approximation, leading to a value of RBE equal to unity.

Going back to the track profile in Fig. 7, the effectiveness may be explained qualitatively from a horizontal line drawn at $\bar{D} = D_{37}\beta^2/z^2_{eff}$. If this line lies above the plateau of the dose profile at the actual a_o, $\bar{D}/D_{37}$ will always be less than 1 for all sensitive elements affected by the ion with no loss in effectiveness; this leads to RBE = 1. If the horizontal line is below the plateau, $\bar{D}/D_{37}$ will be greater than unity with resulting overkill and waste of energy in a part of the sensitive elements. By the same analogy as before, we see that for $\bar{D}(z,\beta, t,a_o) >> D_{37}$, σ_T is less than $\bar{D}/D_{37}$ leading to a value of RBE below unity.

The radiation sensitivity for different ions, k_i, as a function of LET and atomic number is shown in Fig. 8. From this figure it follows that k_i is a multi-valued function of LET which again points to LET as a poor parameter for describing radiation sensitivity.

When considering a thick target, where the ion either loses a major part of its energy or is brought to a complete stop, it is necessary to perform a track segment calculation. In this method the target is divided into a number of segments within which the effective charge and relative velocity may be considered as constant. For each segment the mean LET, the inactivation cross-section σ_T, the energy deposited E_T, and RBE may be calculated. The total RBE for the target is calculated as the mean RBE over all segments, where the RBE for each segment is weighted with the energy deposited in the segment in proportion to the total energy lost in the target.

4. EFFECT OF HIGH-LET RADIATION ON BIOLOGICAL SYSTEMS

The simple exponential character of the dose-response curve for gamma-rays used for physical detectors assumes that the inacti-

vation probability is independent of previous radiation history. This means, e.g. that the response to a total dose D is the same whether the dose is given as a single dose or in several fractions over a time span that is short compared with the physical stability of the detector. This property is used in integrating dose meters in radiation protection.

These detectors will be 1-hit detectors, i.e. a single electron passing through the sensitive area may activate it. Such a detector shows no dose-rate effect and the particular effect of a particle beam may be described by a cross-section, with the total effect calculated as the product of the effect of a single particle times the number of particles in the beam.

Some physical detectors and most biological systems show a more complex dose-response curve. This may be ascribed to the requirement that either the target must be hit more than once by electrons in order for inactivation to occur or there are several targets that must be hit and inactivated. Examples in the field of physical detectors include some of the glow-curve peaks[5] in LiF-TLD and some photographic emulsions[6].

In the multi-hit single-target model the inactivation probability is given by

$$P(z,\beta,t,a_0) = [1- \exp(-\tilde{D}(z,\beta,t,a_0)/D_{37})]^m \qquad (10)$$

with m being an integral number larger than 1, Fig. 9. As is customary in radiation biology, instead of P we may calculate the surviving fraction by the equation

$$S = 1-P(z,\beta,t,a_0) = 1-[1- \exp(\bar{D}(z,\beta,t,a_0)/D_{37})]^m \qquad (11)$$

A typical survival curve for a biological cell system is shown in Fig. 10.

The sigmoid curve in Fig. 9 clearly demonstrates that in contrast to a physical detector the response to a given total dose depends on the number of fractions used to give the dose. Experimental evidence shows that the response decreases with the number of fractions for a given total dose.

Biological systems normally exhibit a dose rate effect with a decrease in effect for a given dose once the dose rate drops below 1 Gy min^{-1}.

The shoulder on the survival curve may be ascribed to an accumulation of sublethal damage corresponding to the inability of a single electron passing through the cell to kill it. This electron may, however, take it to a metastable state which may proceed to inactivation by further absorption of energy from one or more electrons. The dose rate effect is probably due to the presence of repair systems which may partially or wholely repair the damage produced by a single electron and thus remove the cell from the metastable state in a competition with total inactivation of the cell by further absorption of energy.

The parameters m and D_{37} can be calculated from the survival curve in Fig. 10. D_{37} is found from the slope of the linear part and m, often called the extrapolation number, by extrapolating the linear region to D = 0 which will give S = m for D = 0.

The survival curve in Fig. 10 is often described by a two-component expression either

$$S = 1-[1- \exp(-(\alpha D+\beta D^2))] \qquad (12)$$

or

$$S = e^{-D/D_1} \times [1-(1-e^{-D/D_2})]^m \qquad (13)$$

The first expression, Eq. 12, is the so-called α-β or Rossi-Kellerer model[7]. α is supposed to be very small relative to β for low-LET radiation so that inactivation or cell-killing occurs by absorption of energy in two independent steps. α is related to the mean lineal dose ($\bar{Y}_D$) over a distance of 1 μm simulating a cell nucleus as the sensitive element. α increases with $\bar{Y}_D$ leading to a relatively large contribution from one-step processes with increasing LET with a corresponding decrease of the shoulder on the survival curve.

Much work has been devoted to the measurement of $\bar{Y}_D$ for different radiation qualities. The model has had some success in correlating changes in $\bar{Y}_D$ with those in α and β. The problems encountered in giving an explanation of the variation of S with LET over a large range in LET have led to increasing complexity in the model[8], while at the same time experiments with soft x-rays[9] (E < 3 keV) have suggested that energy deposition over a distance of a few nm should be used in the calculation and measurement of $\bar{Y}_D$. The model may be fitted to a large amount of data, but has little predictive value.

The other two-component model, Eq. 13, is often used in radiobiology. In opposition to this model it may be said that if $D_1/D_2 > 0.1$ the single-step mechanism is dominant for all values of D; this leads to an RBE never larger than unity. On the other hand, the term e^{-D/D_1} has no influence if $D_1/D_2 < 0.02$. The model gives no indication of how D_1 and D_2 varies with LET.

Both two-component models, Eqs. 12 and 13, divide the damage to cells into two types: one type which may be repaired (cf. the shoulder on the survival curve and the term $1-[1-e^{-D/D_{37}}]^m$), and a second type called irreparable damage.

The Cohen-model[10], Eq. 13, for calculating effects from radiotherapy at low-LET assumes that D_1/D_2 is 0.5 with about 1/3 of the cells killed in a single-step process[11].

The Rossi-Kellerer model, Eq. 12, assumes that for irreparable

damage to occur two sublethal events have to exist within a distance of 1 μm. A fuller description of the Rossi-Kellerer model and microdosimetry may be found in the literature[7,8,9].

Recognizing the shortcomings of the Rossi-Kellerer model, Katz has developed his track structure model[3] to encompass biological systems. The point of view is again a two-component model. By analogy with particle tracks in emulsions, Katz uses the name ion-kill for a process, where cell-killing occurs following the passage of a single particle through a cell, or alternatively the cell lies so close to the ion path that killing is effected by the tangle of δ-rays ejected from the ion track. The probability for ion-kill may be described by a cross-section.

Biological systems may alternatively accumulate sublethal damage corresponding to the requirement that several targets in the cell must be hit in order that the damage be expressed. Cells may be killed by being hit by δ-rays from two or more different particles. This mode is called gamma-kill with an obvious analogy to low-LET radiation which mainly causes damage in this manner.

Mathematically this may be expressed by the equation

$$P = \pi_i \cdot \pi_\gamma \tag{14}$$

with π_i = probability for ion-kill and π_γ = probability for gamma-kill. π_γ is given as

$$\pi_\gamma = [1 - \exp(-(1-A)D/D_{37})]^m \tag{15}$$

with A equal to the fraction of energy deposited in an ion-kill mode. Similarly π_i may be given by

$$\pi_i = 1-e^{-\sigma D/L} \quad , \tag{16}$$

where L is the LET for the ion. σ may be calculated as already described for physical detectors

$$\sigma(z,\beta,a_0,D_{37},m) = 2\pi \int_0^{t_{max}} P(z,\beta,t,a_0,D_{37},m)\,t\,dt \quad , \tag{17}$$

with

$$P(z,\beta,t,a_0,D_{37},m) = 1- \exp[-D(z,\beta,t,a_0)/D_{37})]^m \quad . \tag{18}$$

The result of this integration is shown in Fig. 11 for different values of z, β and m, with σ/a_0^2 as a function of $z^2/\kappa\beta^2$. κ is related to the physical dimension of the cell and combines multiplicative factors in $\bar{D}$ [12].

It is evident in the figure that the envelope for the multi-hit curves ($m \geq 2$) changes slope with increasing $z^2/\kappa\beta^2$ and reaches a plateau value $\sigma_0 \simeq 1.4\pi a_0^2$ at $z^2/\kappa\beta^2 = 4$ corresponding to the value where the track in the emulsion changes from grain-count to track-width. In cellular systems track-width is analogous to the deposition of all energy in the ion-kill mode, i.e. A=1. For $z^2/\kappa\beta^2 < 1$, σ may be approximated by

$$\sigma(z,\beta,a_0,D_{37},m) = \sigma_0 \cdot [1- \exp(-z^2/\kappa\beta^2)]^m \tag{19}$$

with $\sigma_0 = 1.4\pi a_0^2$.

Both theory and experiment give values of σ_0 that in most cases differ by an order of magnitude from the geometrical cross-section of the cell or cell nucleus. This has lead Katz to treat

σ_0 as a cellular parameter and to assume that Fig. 11 gives a satisfactory description of the relative variation of σ.

In the model for describing the survival curve we now have four cellular parameters σ_0, κ, D_{37}, and m, which together with the ion parameters z and β determine A and σ. However, it must be pointed out that it is not possible to separate ion- and cellular-parameters since all are needed in the calculation of the dose distribution and implicity of A. Katz rightly points out that this eliminates the possibility of describing high- and low-LET radiation without specifying which cellular system is considered. This follows directly from the equation for A

$$A = [1 - \exp(-z^2/\kappa\beta^2)]^m \tag{20}$$

At low values of A we are dealing only with gamma-kill, i.e. the radiation is equivalent to low-LET radiation. With the same values of z and β in another cell system we may have A=1, i.e. only ion-kill. This example demonstrates the futility of distinguishing low- and high-LET radiation.

The cellular parameters D_{37} and m can be calculated from survival curves following gamma-radiation. σ_0 and κ may be calculated from survival curves in experiments with heavy ion irradiation through the equations

$$-\left(\frac{dS}{dD}\right)_{D \to 0} = \frac{\sigma}{L} \tag{21}$$

$$-\left(\frac{dS}{dD}\right)_{D \to \infty} = \frac{\sigma}{L} + (1-A) \cdot D_{37} \tag{22}$$

From A, z, and β, κ and σ_0 may be calculated from these equations. As an example of the use of this method, Fig. 12 shows how the model may be fitted to experimental data.

The functional expression for the dose-response curve allows the calculation of two important biological parameters RBE and OER (Oxygen Enhancement Ratio), and their variation with LET.

To illustrate the problems associated with RBE, Fig. 13 shows survival curves for low- and high-LET radiation with A=0.2 for the same cell system. It is evident that RBE increases with decreasing dose. This is due to the shoulder on the low-LET survival curve, whereas the high-LET curve is almost purely mono-exponential. The increase in RBE is due to the ion-kill process. For a fixed dose RBE will increase with z^2/β^2 until a maximum RBE is reached at $A \simeq 0.5$, when approximately equal amounts of energy are absorbed in the two modes. At still higher values of z^2/β^2, $A \to 1$ and RBE decreases due to over-kill close to the ion path as exemplified in the description of the physical model. Close to the ion path the energy deposited will be much higher than necessary for cell-killing. This is analogous to the track-width regime in emulsions. The decrease in RBE at very high LET may be seen in Fig. 12.

From a comparison of the expressions for survival at high-LET

$$S = [\exp(-\sigma D/L)] \cdot [1-[1- \exp(-(1-A) \cdot D/D_{37})]^m] \qquad (23)$$

and at low-LET

$$S = 1-[1- \exp(-D/D_{37})]^m \qquad (24)$$

it is clear that RBE will increase with decreasing D. In the Rossi-Kellerer model[7] RBE varies in proportion to $D^{-0.5}$. Studies of RBE at low neutron doses give very high values up to 400 for cataract formation in mice[13]. The variation of RBE with dose in these studies may be simulated by track structure theory using cellular parameters of Hela cells.

This increase in RBE at low doses is of paramount importance in the context of radiation protection. Since it is difficult to measure the effect of low-LET radiation at low doses the RBE concept loses much of its value.

At high-LET radiation with $A \approx 1$ a linear extrapolation is possible from high to low doses since the damage occurs along the particle track and the only observable difference between high and low doses is the number of tracks. With low-LET radiation where only gamma-kill exists the cell must be hit more than once. This leads to, e.g., a quadratic extrapolation from high to low doses and a generally much lower risk at lower doses than with the usual linear extrapolation used in radiation protection. A thorough review of RBE for neutrons is found in ref. 14.

The oxygen enhancement ratio denotes that at low-LET D_{37} is approximately 3 times higher when cells are irradiated under normal oxygen tension than when irradiation is carried out under anaerobic conditions. The final explanation of the oxygen effect is not possible at present. However, the main opinion is that it is due to competition between oxygen, which is a biradical, and repair systems containing molecules with sulphydryl groups for reaction with radicals formed by radiation. If O_2 reacts with the radicals peroxy-radicals are formed which cannot be repaired.

The oxygen-effect at high-LET radiation is due to the gamma-kill mode and it follows that OER will decrease with increasing LET. For a given cellular system and an ion beam with known z and β the OER may be calculated from the ratio of the slopes of the survival curves at high doses expressed by Eq. 22. This leads to the following equation

$$OER = \frac{\sigma_N/L + (1-A)D_{37}^{N}}{\sigma_{O_2}/L + (1-A)D_{37}^{O_2}} \qquad (25)$$

with the subscripts N and O_2 used for irradiation carried out under nitrogen and oxygen, respectively. σ_N and σ_{O_2} are identical. This follows directly from the equation for σ. When A=1, OER becomes equal to 1.

The lower OER of high-LET radiation is the main drive behind the application of high-LET radiation in radiation therapy of cancer since many tumors are presumed to contain a considerable number of hypoxic cells. These cells will be radiation resistant, requiring doses for eradication far above what normal tissue will tolerate. There is no biological basis for assuming that cancerous tissues will have an RBE different from normal tissues, disregarding possible differences in the OER.

The equations for ion- and gamma-kill are valid only for monoenergetic ions. This is an ideal case not found in practice because of the energy dispersion present after the traversal through only a few μm of tissue.

This problem may be solved mathematically by dividing the energy spectrum into a series of discrete components homogeneous in z and β. The total ion-kill probability will be the product of this probability for these separate and independent components. The total gamma-kill probability is calculated from the total dose deposited in the gamma-kill mode; it may be summarized from the separate components inclusive of an eventual contamination of the beam with γ-rays. Since the total cell-killing probability is given by $\pi_i \cdot \pi_\gamma$ the survival S is given by

$$S = [\exp(-\sigma_0 \Sigma_j A_j \cdot F_j)] \cdot [1-[1- \exp(-\Sigma_j (1-A_j) \cdot D_j/D_{37})]^m] \quad (26)$$

where A_j equals the proportion of the dose deposited by component j in the ion-kill mode and F_j equals the flux of component j.

This formalism can account for the slowing down of a heavy ion beam including secondary particles. It may also be used for neutrons with known energy spectra of secondary, tertiary, quarternary, etc. particles.

In many respects this formalism is too unhandy. The situation may be simplified by the introduction of an equivalent radiation field. This is defined as having the same π_i, π_γ, and D (total dose) as the mixed field. The equivalent field is only a computational simplification and may be impossible to realize. An important advantage of this method is that it becomes much easier to simulate the effect of mixing the high-LET field with γ-rays. This modality is used in many of the present treatment protocols for neutron therapy, and the equivalent field simplifies the calculation of the optimal mixture of the two radiation types.

REFERENCES

1) Mozumder, A. and J.L. Magee (1966). Theory of Radiation Chemistry, VII. Structure and Reactions in Low LET Tracks. J. Chem. Phys. 45, 3332-3341.

2) Katz, R., B. Ackerson, M. Homayoonfar and S.C. Sharma (1971). Inactivation of Cells by Heavy Ion Bombardment. Radiat. Res. 47, 402-425.

3) Katz, R., S.C. Sharma and M. Homayoonfar (1972). The Structure of Particle Tracks. F.H. Attix (ed.). Topics in Radiation Dosimetry, Suppl. 1, 317-383 (Academic Press, N.Y.).

4) Dertinger, H. and H. Jung (1970). Molecular Radiation Biology. Ch. 5 (Springer, Berlin).

5) Waligórski, M.P.R. and R Katz (1980). Supralinearity of Peak 5 and Peak 6 in TLD-700. Nucl. Instrum. Methods 172, 463-470.

6) Katz, R. and E.C. Pennington (1978). Radiobiological Aspects of Supralinear Photographic Emulsions. Phys. Med. Biol. 23, 1115-1123.

7) Kellerer, A.M. and H.H. Rossi (1972). The Theory of Dual Radiation Action. Curr. Top. Rad. Res. Quart. 8, 85-158.

8) Kellerer, A.M. and H.H. Rossi (1978). A Generalized Formulation of Dual Radiation Action. Radiat. Res. 75, 471-488.

9) Goodhead, D.T. (1977). Inactivation and Mutation of Cultured Mammalian Cells by Aluminium Characteristic Ultrasoft X-Rays. III. Implications for Theory of Dual Radiation Action. Int. J. Radiat. Biol. 32, 43-70.

10) Cohen, L. (1971). A Cell Population Kinetic Model for Fractionated Radiation Therapy. I. Normal Tissues. Radiology 101, 419-427.

11) Cohen, L. (1973). Cell Population Kinetics in Radiation Therapy: Optimazation of Tumor Dosage. Cancer 32, 236-244.

12) Katz, R., B. Ackerson, M. Homayoonfar and S.C. Sharma (1971). Inactivation of Cells by Heavy Ion Bombardment. Radiat. Res. 47, 402-425.

13) Bateman, J.L., H.H. Rossi, A.M. Kellerer, C.V. Robinson and V.P. Bond (1972). Dose-Dependence of Fast Neutron RBE for LENS Opacification in Mice. Radiat. Res. 51, 381-390.

14) Katz, R. and S.C. Sharma (1975). RBE-Dose Relations for Neutrons and Pions. Phys. Med. Biol. 20, 410-419.

LIST OF FIGURES

Fig. 10. Surviving fraction as a function of radiation dose.

Fig. 11. Inactivation cross-section as a function of $z^2/\kappa\beta^2$ with the extrapolation number m as a parameter. For the sake of clarity the curves are displaced by the exponent s on the vertical axis.

Fig. 12. Surviving fraction of Chinese hamster cells as a function of radiation dose with z and β as parameters. For the sake of clarity the curves are displaced by a factor s on the horizontal axis.

Fig. 13. Surviving fraction of human kidney cells as a function of radiation dose from 200 kV_p X-rays (A=0) and 5.2 MeV α-particles (A=0.2).

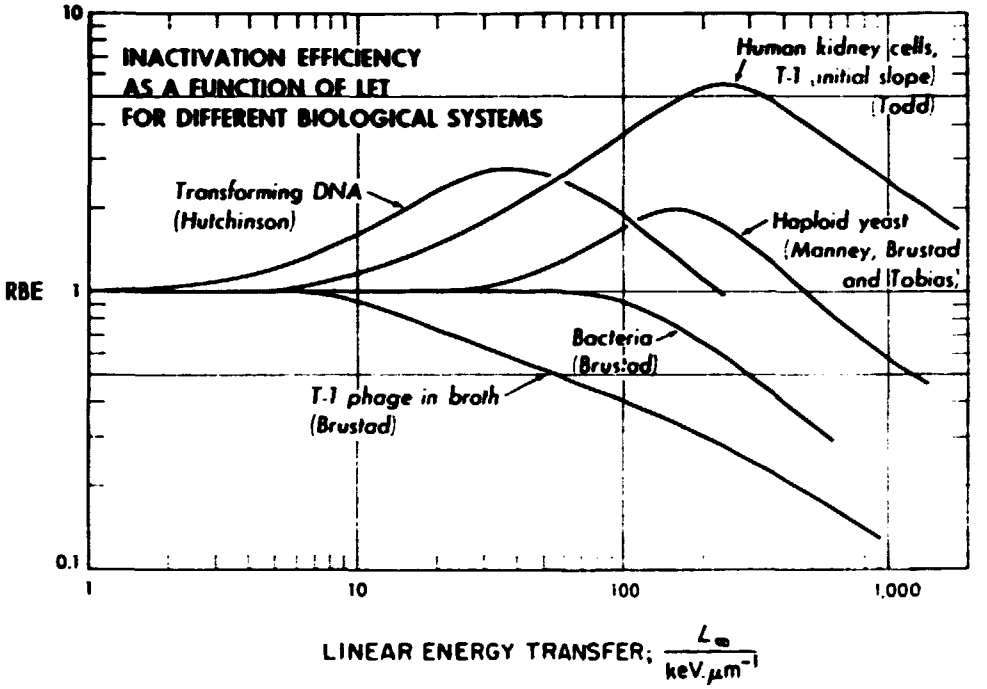

Fig. 1. RBE versus LET for some biological systems.

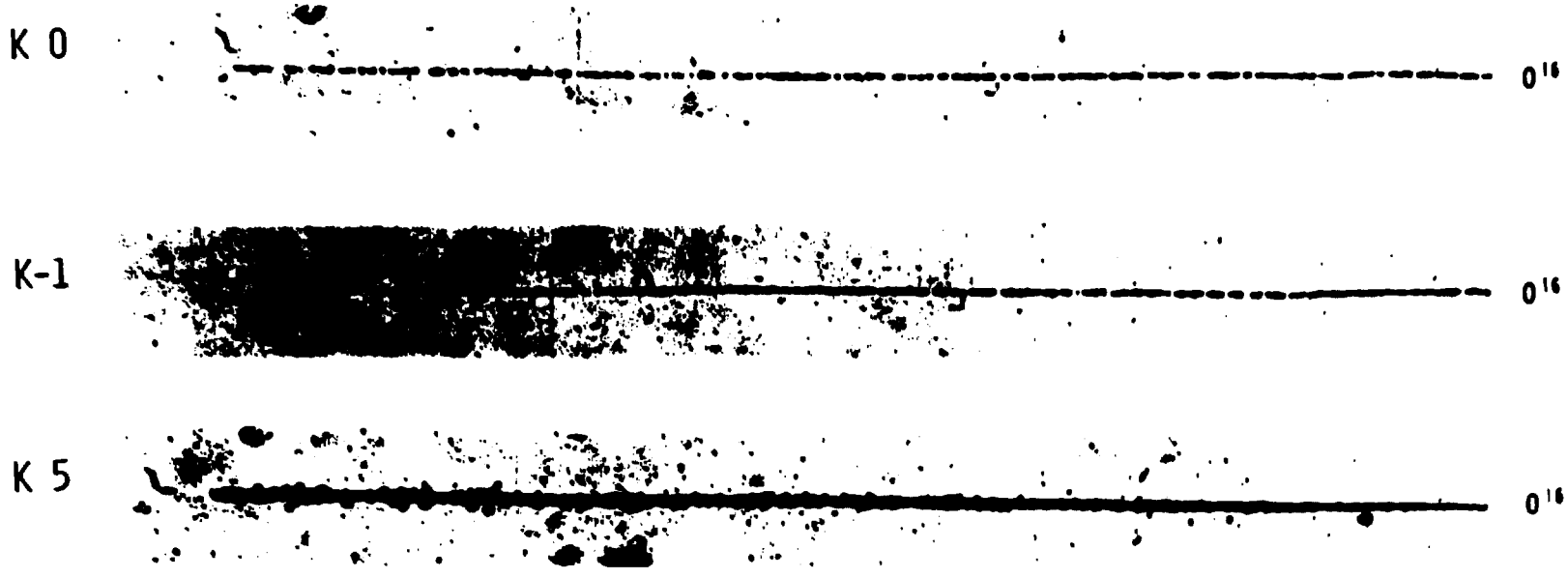

Fig. 2. Tracks from an oxygen ion in photographic emulsions of differing radiation sensitivities. K5 is the most sensitive emulsion.

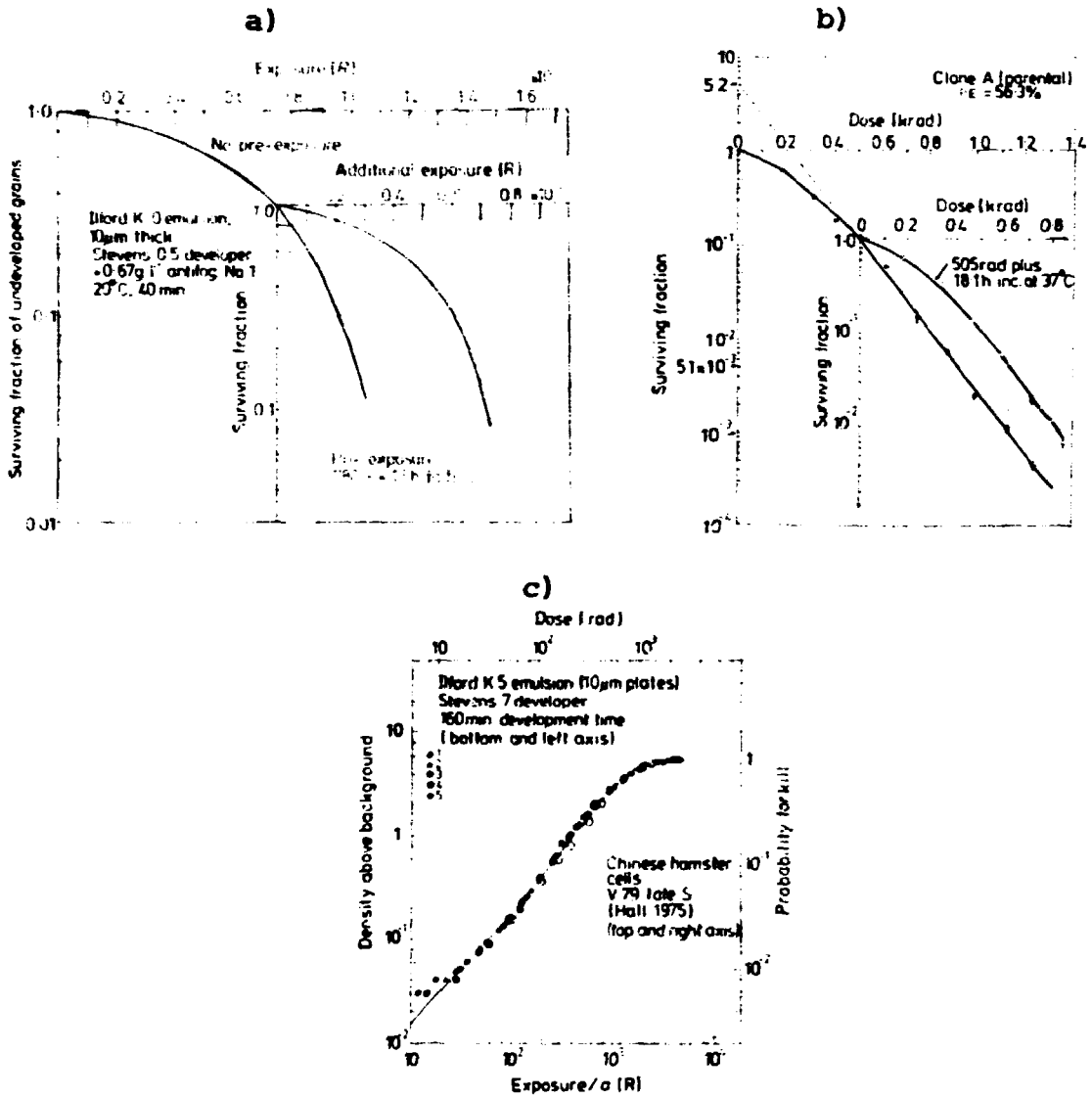

Fig. 3. a) Photographic emulsion simulating the radiation sensitivity of a biological system for a fractionated dose.
b) Surviving fraction of hamster cells as a function of fractionated dose.
c) Supra-linearity in radiation sensitivity for a photographic emulsion (solid line) compared with experimental data for survival of hamster cells.

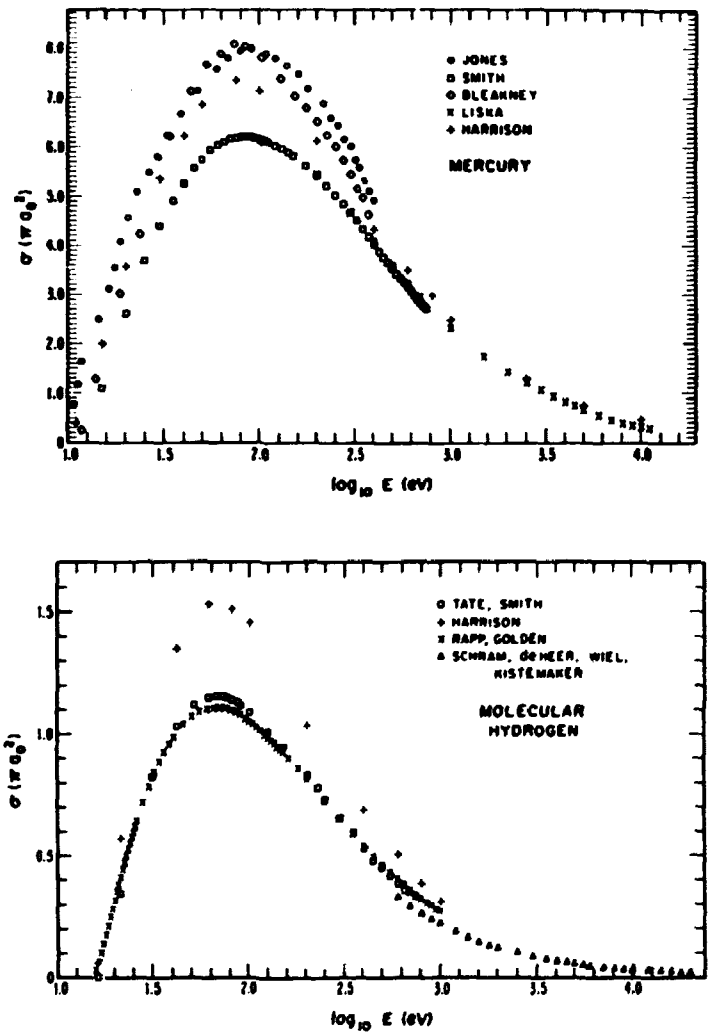

Fig. 4. Electron ionization cross-sections of mercury and molecular hydrogen.

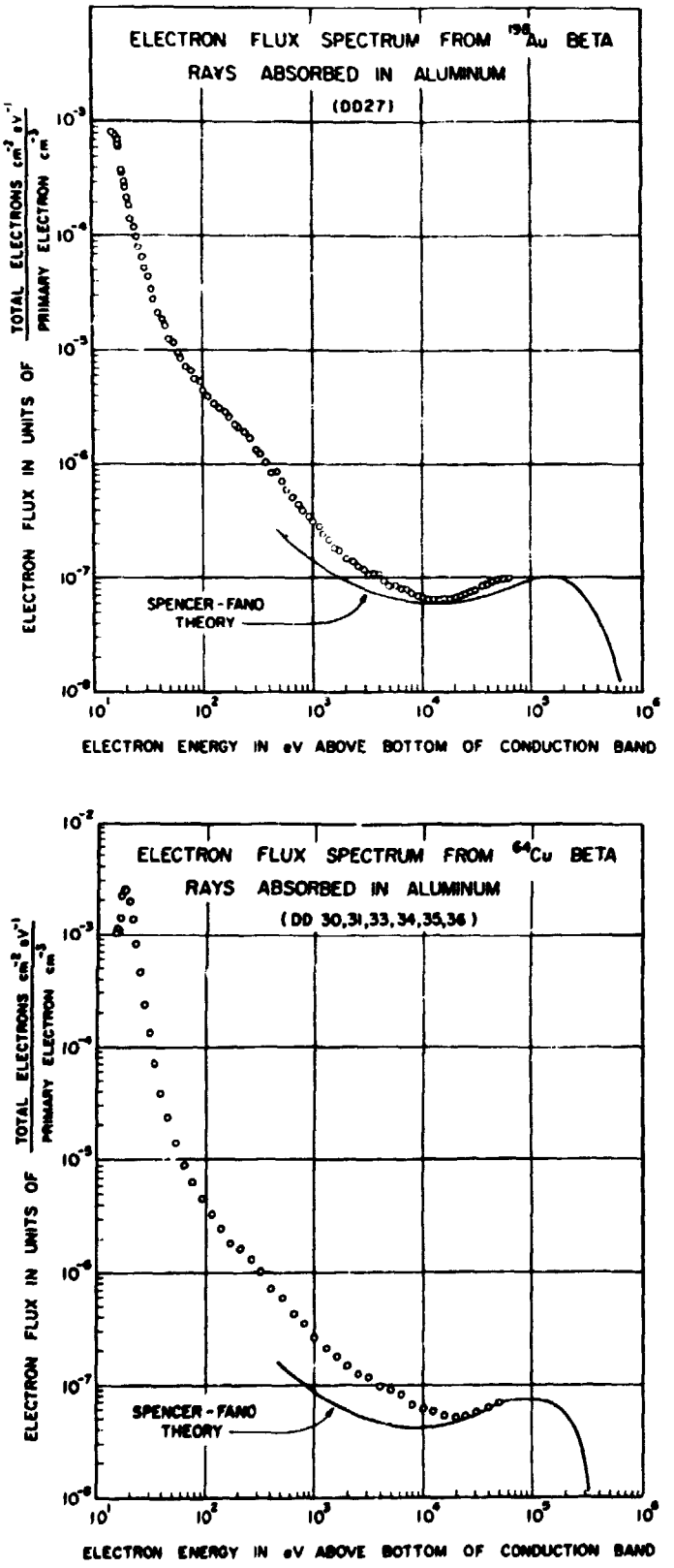

Fig. 5. Electron flux spectra from ^{198}Au and ^{64}Cu β-rays in aluminium.

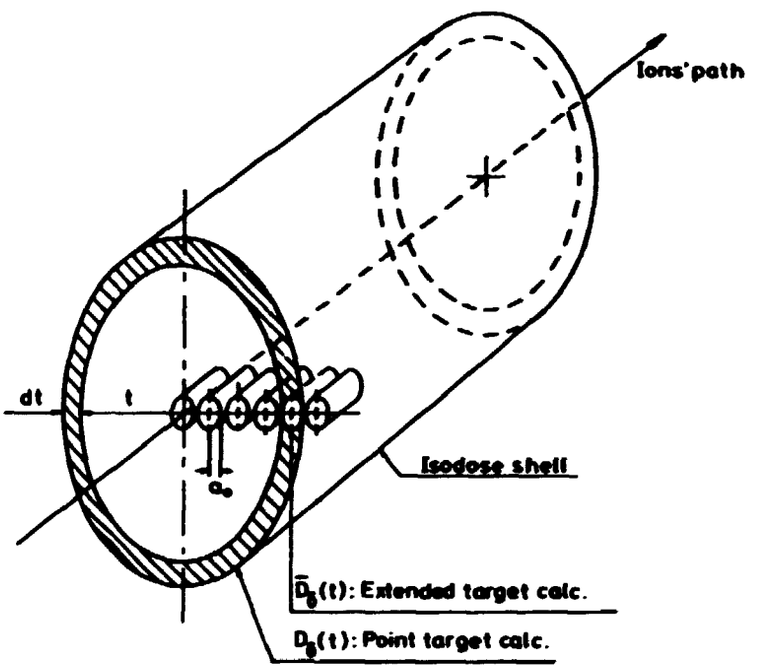

Fig. 6. Schematic representation of the radiation sensitive elements around the path of an ion for calculation of the extended target dose.

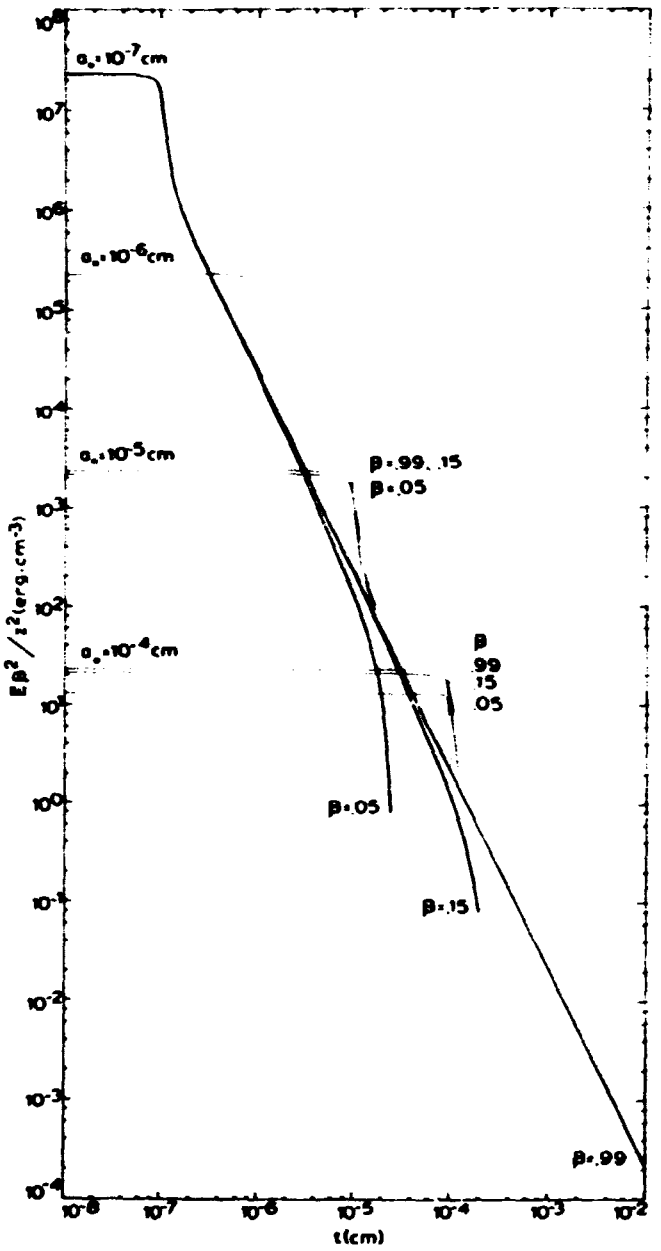

Fig. 7. Mean dose deposited in the radiation sensitive element as a function of the radial distance t from the axis of the path of an ion. Parameters are the radius (a_o) of the sensitive element and the ion velocity (β) relative to that of light.

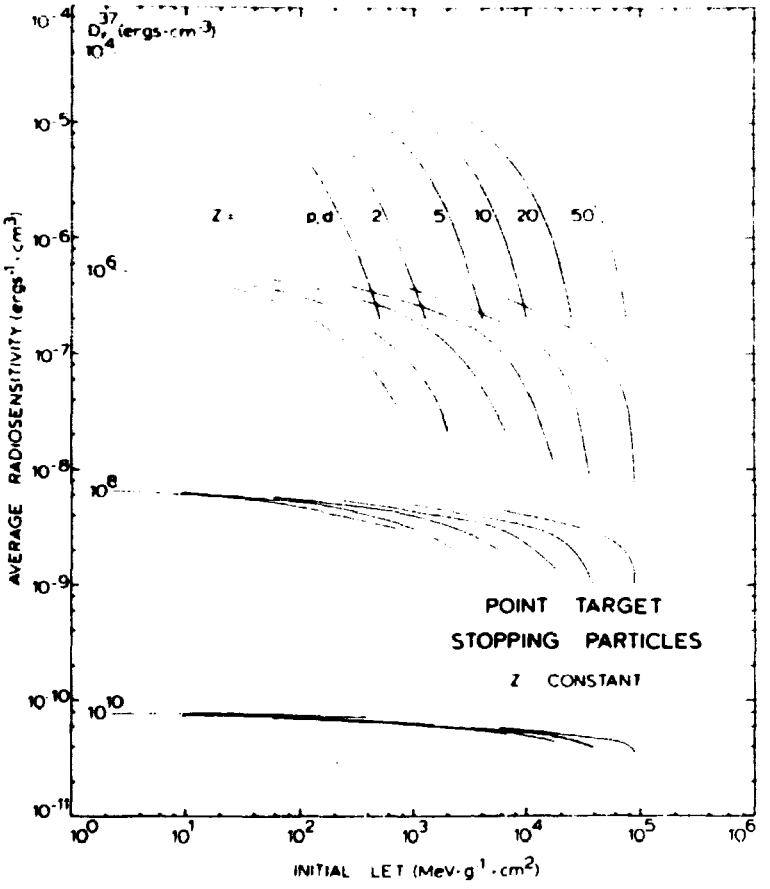

Fig. 8. Radiation sensitivity k_i as a function of LET with D_{37} and atomic number of the ion as parameters.

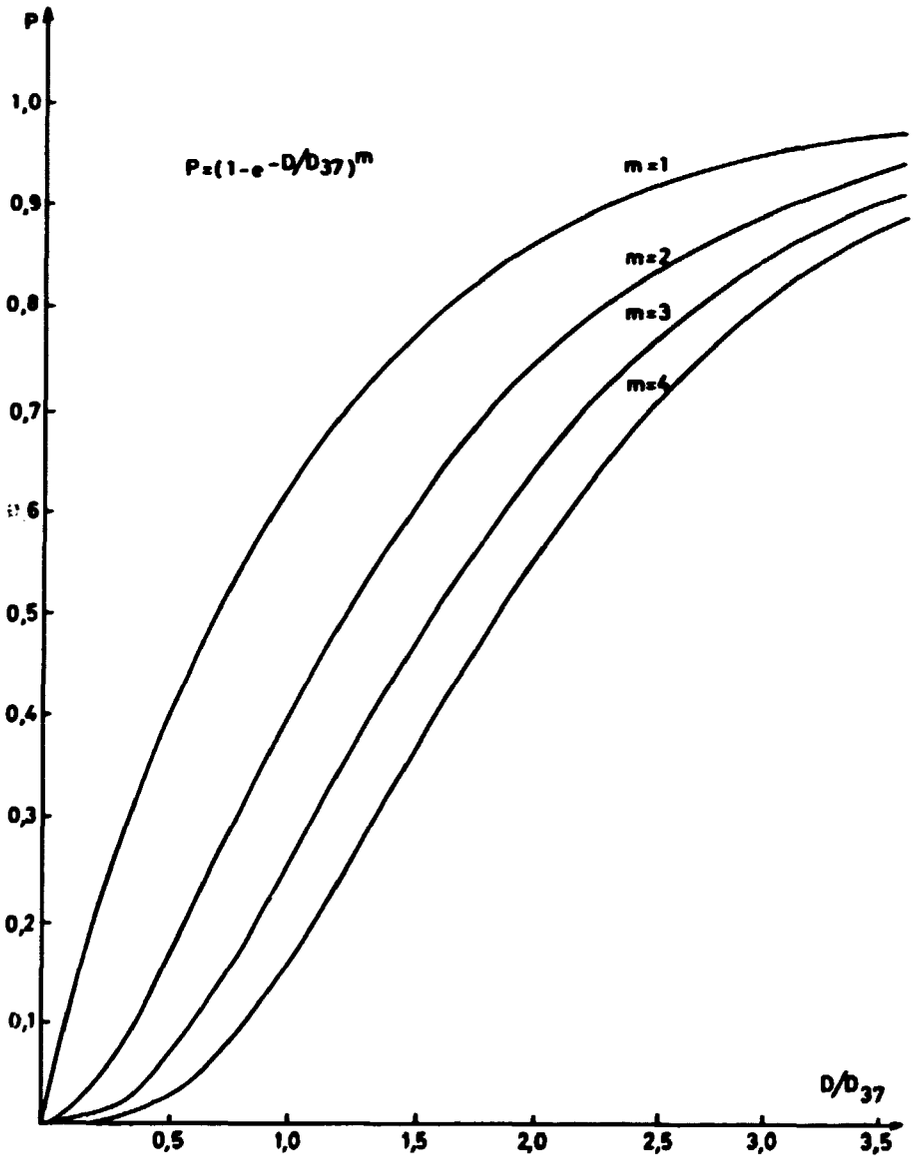

Fig. 9. Inactivation probability P as a function of normalized dose D/D_{37} with the extrapolation number m as a parameter.

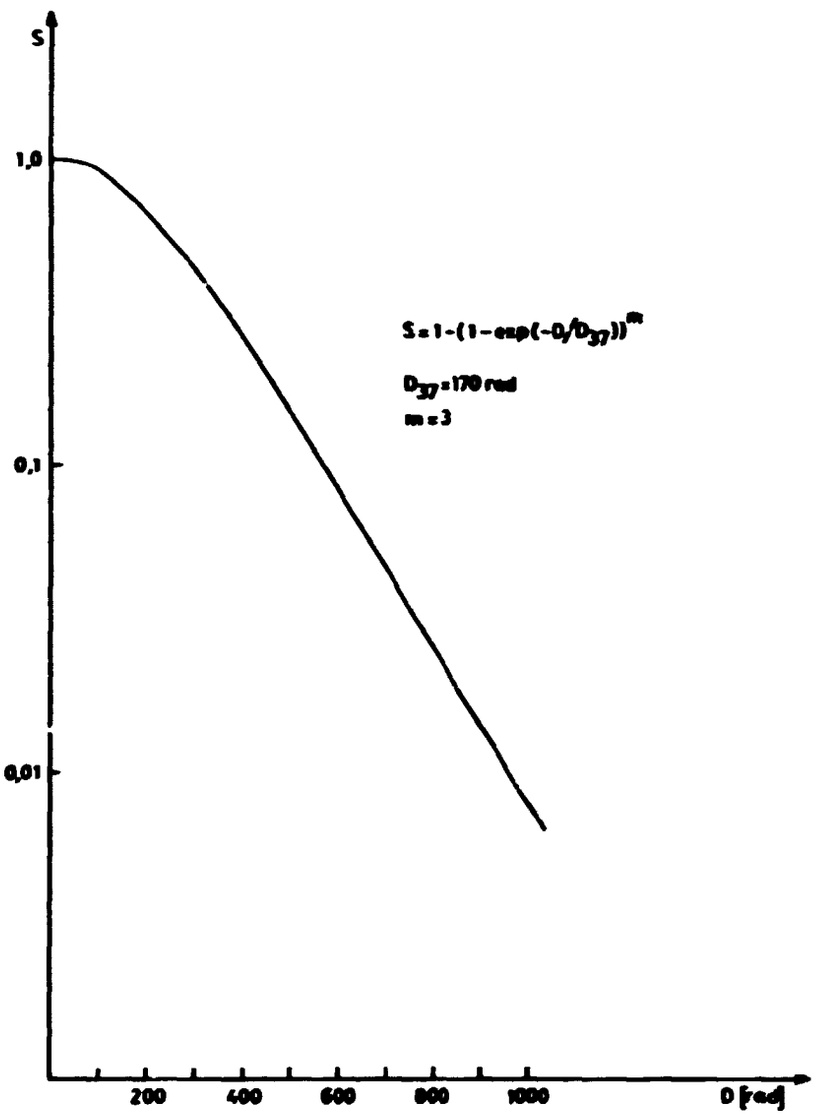

Fig. 10. Surviving fraction as a function of radiation dose.

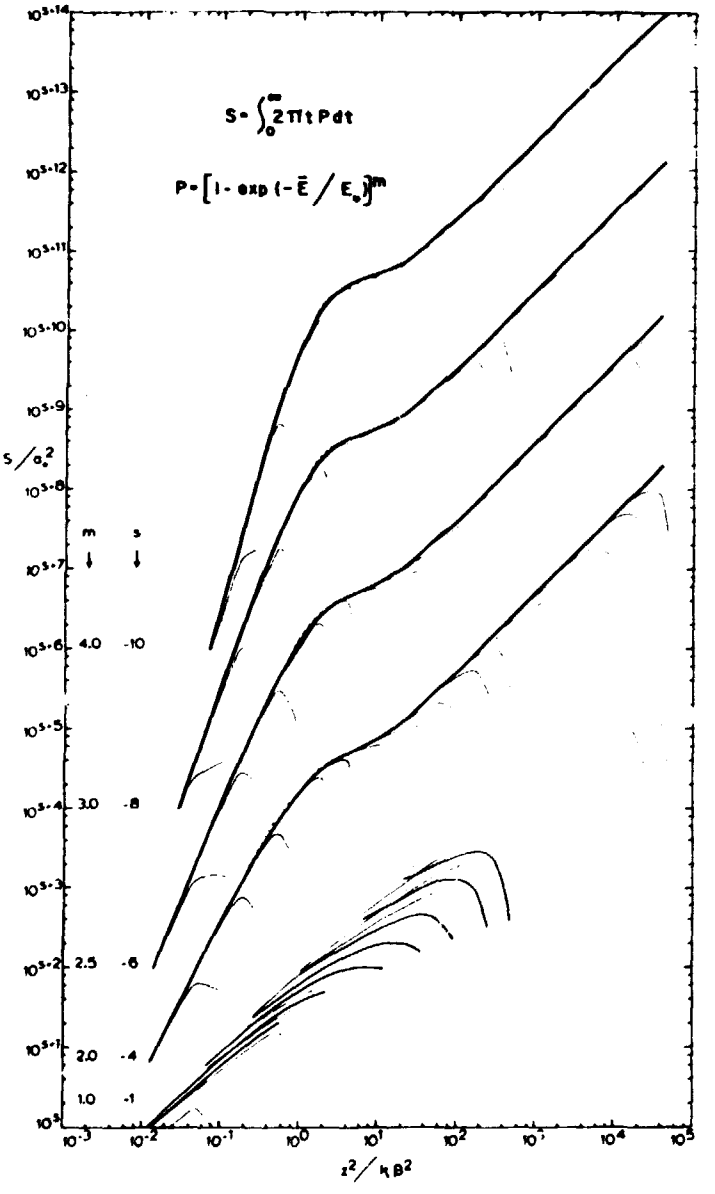

Fig. 11. Inactivation cross-section as a function of $z^2/\kappa\beta^2$ with the extrapolation number m as a parameter. For the sake of clarity the curves are displaced by the exponent s on the vertical axis.

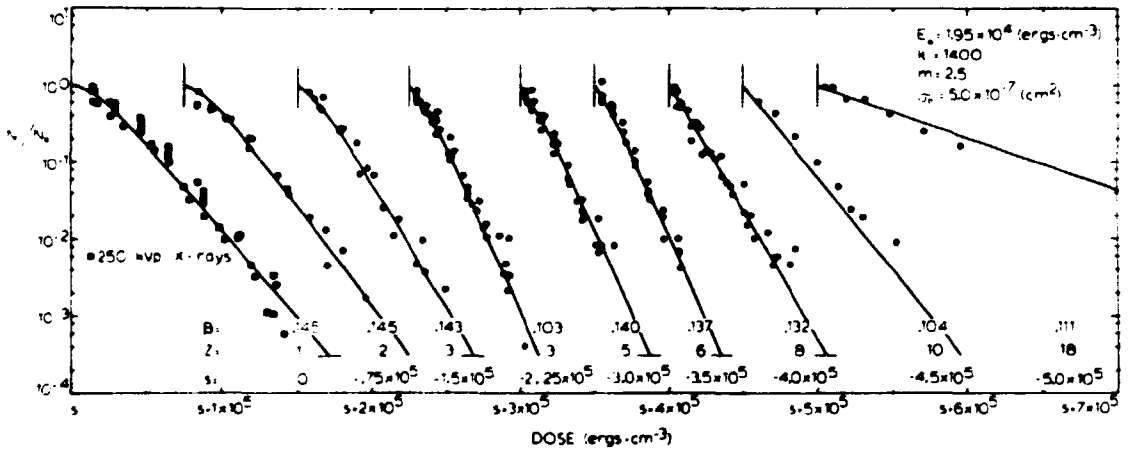

Fig. 12. Surviving fraction of Chinese hamster cells as a function of radiation dose with z and β as parameters. For the sake of clarity the curves are displaced by a factor s on the horizontal axis.

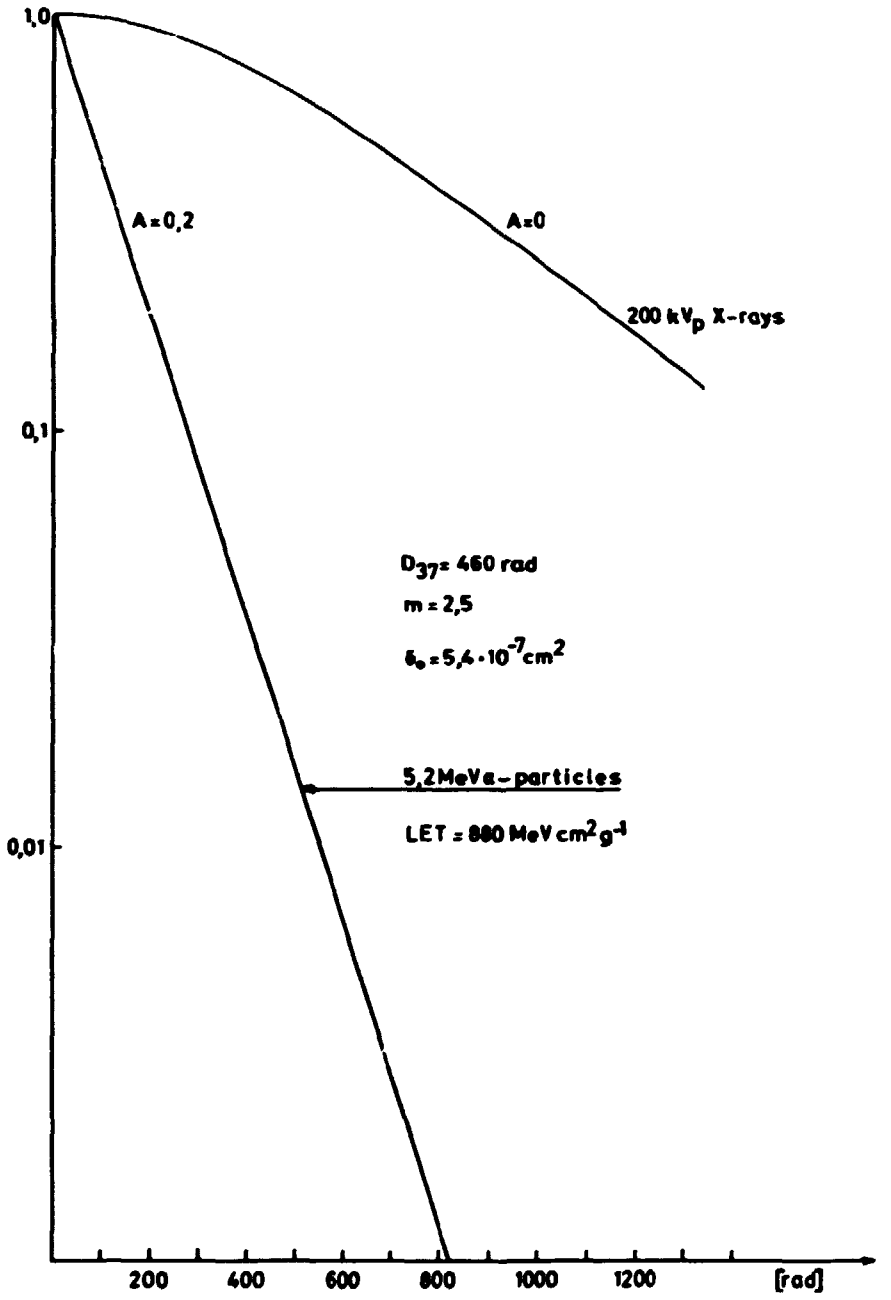

Fig. 13. Surviving fraction of human kidney cells as a function of radiation dose from 200 kV_p X-rays (A=0) and 5.2 MeV α-particles (A=0.2).

Sales distributors:
Jul. Gjellerup, Sølvgade 87,
DK-1307 Copenhagen K, Denmark

Available on exchange from:
Risø Library, Risø National Laboratory,
P.O.Box 49, DK-4000 Roskilde, Denmark

ISBN 87-550-0886-0
ISSN 0106-2840